A Stable Simplification of a Fas-signaling Pathway Model for Apoptosis

Ya-Jing Huang
Zhou Pei-Yuan Center for Appl. Math.
Tsinghua Univ., Beijing 100084, China
Email: huangyj09@mails.tsinghua.edu.cn

Wen-An Yong
Zhou Pei-Yuan Center for Appl. Math.
Tsinghua Univ., Beijing 100084, China
Email: wayong@tsinghua.edu.cn

***Abstract*—Apoptosis is important for maintaining normal embryonic development, tissue homeostasis and normal immune-system operation in multicellular organisms. Its malfunction may result in serious diseases such as cancer, autoimmunity, and neurodegeneration. In apoptosis, tens of species are present in many biochemical reactions with times scales of widely differing orders of magnitude. According to the law of mass action, apoptosis is usually described with a large and stiff system of ODEs (ordinary differential equations). The goal of this work is to derive a simple system of ODEs by using the classical PEA (partial equilibrium approximation) method. For this purpose, we firstly justify the mathematical correctness of the PEA in a quite general framework. On the basis of this result, we simplify the Fas-signaling pathway model proposed by Hua et al. (2005) by assuming the fastness of several reversible reactions. Numerical simulations and sensitivity analysis show that our simplification model is reliable.**

Keywords: Apoptosis, partial equilibrium approximation, singular perturbation theory, the principle of detailed balance

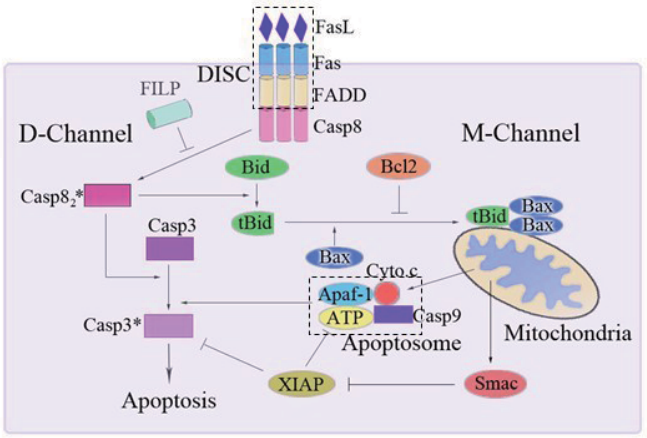

Fig. 1. The Fas-induced apoptotic pathway, including two channels.

I. Introduction

Apoptosis is one of the most basic biological processes. It is a form of programmed cell death (PCD) and is an everyday occurrence in tissue turnover. In apoptosis, superfluous and potentially dangerous cells in multicellular organisms are removed. This genetically regulated process ensures normal embryonic development, tissue homeostasis and normal immune-system operation in multicellular organisms, including humans. On the other hand, malfunction of apoptosis may result in serious diseases such as cancer, autoimmunity, and neurodegeneration [1], [2], [3], [4], [5]. For these reasons, understanding the mechanism of apoptosis is of fundamental importance.

Apoptotic cell death is triggered by extrinsic, receptor-mediated, or intrinsic, mitochondria-mediated, signalling pathways that induce death-associated proteolytic and/or nucleolytic activities. The intrinsic pathway can be initiated by many kinds of factors like the UV or genotoxic stress, which lead to the damage of the cell. The extrinsic pathway is activated by the death receptors such as TNF-R1(DR1,p55), Fas(DR2,CD95), DR3(APO-3,TRAMP), DR4(APO-2,TRAIL-R1) and DR5(TRICK2,TRAOL-R2) [1], [6], [7], [8].

The Fas signaling-induced pathway is the best characterized and is schematically shown in Fig. 1. It begins with the binding of Fas ligands (FasL), Fas and FADD (Fas-associated death domain) to form the complex DISC (death-inducing signaling complex). The latter can recruits initiator caspases such as caspase-8 (Casp8) molecules to cleave and activate them. The activated initiator caspase (Casp8_2^*) can cleaves and activates the executor caspase-3 (Casp3) to form Casp3* directly. The amount of Cas3* is regarded as the indicator of apoptosis. This way to activate Casp3 is called D-channel. In addition, Casp3 can also be activated in a so-called M-channel. In this channel, Casp8_2^* acts as an enzyme and cleaves Bid to generate truncated (t)Bid. The tBid then binds to two molecules of Bax to form a complex tBid:Bax_2, which will induce the release of Cyto.c and Smac from the mitochondria. The released Cyto.c* will combine an adaptor protein Apaf-1, ATP and caspase-9 to form apoptosome and thereby activate caspase-9. The activated caspase-9 (Casp9*) cleaves and activates Casp3. Here, besides Casp8_2^*, the apoptosome and Casp9* act as enzymes as well. On the other hand, the M-channel can be blocked by XIAP (X-linked inhibitor of apoptosis protein) and Bcl2 through their bindings to the released Smac*, Casp9, Casp3*, Bax and tBid. For apoptosis of human tumor T cells, a detailed reaction network has been given by Hua et al. in [9], with complete reaction rate constants and initial data (see Tables I and II below). By the way, Hua et al. obtained a conclusion, consistent with previous experiments, that the effects of D-

978-1-4673-4398-5/12/$31.00 ©2012 IEEE

channel and M-channel can be altered by varying the amount of Casp8$_2^*$ generated by DISC [10], [11], [12].

The above description indicates the complexity of the apoptotic process. Indeed, this process involves tens of molecules (species) and many many biochemical reactions. Once the law of mass action [13] is employed, the process corresponds to a simultaneous system of tens of ordinary differential equations (ODEs). Such a large scale system of ODEs can hardly help us to understand the mechanism of the apoptosis. It also prohibits powerful mathematical treatments, including numerical ones.

The goal of this work is to present a mathematically effective reduction of the large system from [9]. Two widely used methods for simplifying (bio-)chemical kinetics mechanisms are the Quasi Steady-State Approximation(QSSA) [14], [15], [16] and Partial Equilibrium Approximation(PEA) [17], [18], [19]. The former assumes that the concentrations of reactive intermediate species stop to change after a very short time [20], while the latter assumes that some reactions are much faster than others [21]. Although the two methods have been used to simplify chemical kinetics mechanisms for many years [13], [22], [23], [24], [25], they seem to lack a systematically mathematical justification. Recently, we pointed out that the PEA method can be rigorously justified for reversible reactions obeying the principle of detailed balance [26], [27], by using the singular perturbation theory of initial value problems for ODEs [28], [29]. Thus, our reduction will base on this justified PEA method and therefore are called to be stable.

In [30], Okazaki et al. derived a simplified model by using both the QSSA and PEA methods together with some empirical assumptions. For their derivation, they firstly divided the whole network into two parts, the DISC subsystem (DSS) and the intracellular-signaling subsystem (ISS), since the function of the DISC subsystem is only supplying Casp8$_2^*$ to the remaining downstream part. Moreover, their simplification neglects the effects of Smac and XIAP, which seems ok for their initial data. In addition, the authors also divided the simultaneous reactions in the ISS part into some independent groups. For example, in applying the QSSA method for the intermediate species Casp8$_2^*$:Casp3 (see formula (A.1) in Appendix A of [30]), they assumed that the concentration sum of Casp8$_2^*$ and Casp8$_2^*$:Casp3 was conserved (A.2) and obtained the Michaelis-Menten equation (A.4) for the product Casp3*. The latter is only true if Casp8$_2^*$ does not participate in other reactions. However, this is not the case here because Casp8$_2^*$ is simultaneously involved in the reactions of generating tBid. Namely, the reactions of generating tBid were considered in [30] to be independent of those for the activation of Casp3 by Casp8$_2^*$. Similar conservation assumptions were used for several steps, while the PEA method is used for a number of reversible reactions. In this way, they simplified the ISS subsystem to obtain a so-called ISS skeleton model. Although the ISS skeleton model may describe the dominant role of Casp8$_2^*$ to the two channels, its derivation seems *ad hoc* and baseless.

In this paper, we use the PEA method and obtain a simplified model from the entire intracellular-signaling subsystem. This simplification is based on the fact that there are large variances in time scales among different reactions, making the ODE system stiff. In doing this, we firstly show, by using different initial data, that Smac and XIAP are often not negligible. Then we check the principle of detailed balance for the fast reactions as a whole and derive our simplified model. Through numerical simulations, we compare this new model with the original ISS model and Okazaki et al.'s skeleton model [30] from various aspects, including accuracy, sensitivity and M-D transition behavior. Moreover, we introduce a new quantity to evaluate the new model. All these numerical results show the reliability of both our simplified model and the PEA method.

However, the present simplification is preliminary and more will be reported in a forthcoming paper. We believe that the framework presented here is useful for simplifying other biochemical systems as well as the apoptosis problem.

The paper is organized as follows. In Section 2 we present the entire ISS and show, by using different initial data, that Smac and XIAP are often not negligible. Section 3 gives details of the simplification from the entire ISS model by checking the principle of detailed balance. Numerical simulations are reported in Section 4. Finally, some conclusions and comments are summarized in Section 5.

II. The Intracellular-signaling Subsystem

The Fas-signaling pathway model proposed by Hua et at. [9] is chemically expressed as in Table 1. As in Okazaki et al.[30], our simplification will be directed to the intracellular-signaling subsystem (ISS)—the downstream process of apoptosis, since this part is quite independent of the upstream process initiated by FasL to activate Casp8. Moreover, we follow [30] and assume that the concentration of ATP is a fixed constant. Thus, there are 28 species and 19 biochemical reactions involved in the downstream process.

According to the law of mass action [13], the dynamics of the ISS is governed by 28 ordinary differential equations

$$\frac{dU}{dt} = Q(U), \tag{1}$$

where U is a column vector with 28 components representing the concentrations of all the 28 species in the ISS:

$$\begin{aligned} U = \ & \big([Casp8_2^*], [Casp8_2^* : Casp3], [Casp8_2^* : Bid], [Bid], \\ & [tBid], [tBid : Bax], [tBid : Bax_2], [Bcl_2 : tBid], \\ & [Bax], [Bcl_2 : Bax], [Bcl_2], [Cyto.c], [Cyto.c^*], \\ & [Cyto.c^* : Apaf : ATP], \\ & [Cyto.c^* : Apaf : ATP : Casp9], \\ & [Cyto.c^* : Apaf : ATP : Casp9_2], \\ & [Apaf], [Casp9^*], [Casp9], [Casp3], \\ & [Casp9* : Casp3], [Casp3^*], [Smac], [Smac^*], \\ & [XIAP], [Smac^* : XIAP], [Casp9 : XIAP], \\ & [Casp3^* : XIAP]\big)^T. \end{aligned}$$

Here $[S]$ denotes the concentration of the substance S. For example, $[Casp8_2^*]$ is the concentration of the substance Casp8$_2^*$. Cyto.c* and Smac* denote Cyto.c and Smac released to cytosol from mitochondrial, respectively, and Apaf stands

978-1-4673-4398-5/12/$31.00 ©2012 IEEE

TABLE I
THE FAS-SIGNALING PATHWAY MODEL DUE TO HUA ET AT. (2005)

Reaction		k_{Hi}	k_{-Hi}
(H1)	$FasL + Fas \underset{k_{-H1}}{\overset{k_{H1}}{\rightleftharpoons}} FasC$	$9.09 \times 10^{-5} nM^{-1} s^{-1}$	1.00×10^{-4}
(H2)	$FasC : FADD_p : Casp8_q : FLIP_r + FADD \underset{k_{-H2}}{\overset{k_{H2}}{\rightleftharpoons}} Fas : FADD_{p+1} : Casp8_q : FILP_r$	$5.00 \times 10^{-4} nM^{-1} s^{-1}$	0.2
(H3)	$FasC : FADD_p : Casp8_q : FILP_r + Casp8 \underset{k_{-H3}}{\overset{k_{H3}}{\rightleftharpoons}} Fas : FADD_p : Casp8_{q+1} : FILP_r$	$3.50 \times 10^{-3} nM^{-1} s^{-1}$	0.018
(H4)	$FasC : FADD_p : Casp8_q : FLIP_r + FILP \underset{k_{-H4}}{\overset{k_{H4}}{\rightleftharpoons}} Fas : FADD_p : Casp8_q : FILP_{r+1}$	$3.50 \times 10^{-3} nM^{-1} s^{-1}$	0.018
(H5)	$FasC : FADD_p : Casp8_q : FLIP_r \xrightarrow{k_{H5}} Casp8*_2 : p41 + FasC : FADD_p : Casp8_{q-1} : FILP_r$	$0.3 s^{-1}$	
(H6)	$Casp8^*_2 : p41 \xrightarrow{k_{H6}} Casp8^*_2$	$0.1 s^{-1}$	
(H7)	$Casp8^*_2 + Casp3 \underset{k_{-H7}}{\overset{k_{H7}}{\rightleftharpoons}} Casp8^*_2 : Casp3$	$1.00 \times 10^{-4} nM^{-1} s^{-1}$	0.06
(H8)	$Casp8^*_2 : Casp3 \xrightarrow{k_{H8}} Casp8^*_2 + Casp3^*$	$0.1 s^{-1}$	
(H9)	$Casp8^*_2 + Bid \underset{k_{-H9}}{\overset{k_{H9}}{\rightleftharpoons}} Casp8^*_2 : Bid$	$5.00 \times 10^{-4} nM^{-1} s^{-1}$	0.005
(H10)	$Casp8^*_2 : Bid \xrightarrow{k_{H10}} Casp8^*_2 + tBid$	$0.1 s^{-1}$	
(H11)	$tBid + Bax \underset{k_{-H11}}{\overset{k_{H11}}{\rightleftharpoons}} tBid : Bax$	$2.00 \times 10^{-4} nM^{-1} s^{-1}$	0.02
(H12)	$tBid : Bax + Bax \underset{k_{-H12}}{\overset{k_{H12}}{\rightleftharpoons}} tBid : Bax_2$	$2.00 \times 10^{-4} nM^{-1} s^{-1}$	0.02
(H13)	$Smac + tBid : Bax_2 \xrightarrow{k_{H13}} Smac^* + tBid : Bax_2$	$1.00 \times 10^{-3} nM^{-1} s^{-1}$	
(H14)	$Smac^* + XIAP \underset{k_{-H14}}{\overset{k_{H14}}{\rightleftharpoons}} Smac^* : XIAP$	$7.00 \times 10^{-3} nM^{-1} s^{-1}$	2.21×10^{-3}
(H15)	$Cyto.c + tBid : Bax_2 \xrightarrow{k_{H15}} Cyto.c^* + tBid : Bax_2$	$1.00 \times 10^{-3} nM^{-1} s^{-1}$	
(H16)	$Cyto.c^* + Apaf + ATP \underset{k_{-H16}}{\overset{k_{H16}}{\rightleftharpoons}} Cyto.c^* : Apaf : ATP$	$2.78 \times 10^{-7} nM^{-1} s^{-1}$	5.70×10^{-3}
(H17)	$Cyto.c^* : Apaf : ATP + Casp9 \underset{k_{-H17}}{\overset{k_{H17}}{\rightleftharpoons}} Cyto.c^* : Apaf : ATP : Casp9$	$2.84 \times 10^{-4} nM^{-1} s^{-1}$	0.07493
(H18)	$Cyto.c^* : Apaf : ATP : Casp9 + Casp9 \underset{k_{-H18}}{\overset{k_{H18}}{\rightleftharpoons}} Cyto.c^* : Apaf : ATP : Casp9_2$	$4.41 \times 10^{-4} nM^{-1} s^{-1}$	0.1
(H19)	$Cyto.c^* : Apaf : ATP : Casp9_2 \xrightarrow{k_{H19}} Cyto.c^* : Apaf : ATP : Casp9 + Casp9^*$	$0.7 s^{-1}$	
(H20)	$Casp9^* + Casp3 \underset{k_{-H20}}{\overset{k_{H20}}{\rightleftharpoons}} Casp9^* : Casp3$	$1.96 \times 10^{-5} nM^{-1} s^{-1}$	0.05707
(H21)	$Casp9^* : Casp3 \xrightarrow{k_{H21}} Casp9^* + Casp3^*$	$4.8 s^{-1}$	
(H22)	$Casp9 + XIAP \underset{k_{-H22}}{\overset{k_{H22}}{\rightleftharpoons}} Casp9 : XIAP$	$1.06 \times 10^{-4} nM^{-1} s^{-1}$	1.00×10^{-3}
(H23)	$Casp3^* + XIAP \underset{k_{-H22}}{\overset{k_{H22}}{\rightleftharpoons}} Casp3^* : XIAP$	$2.47 \times 10^{-3} nM^{-1} s^{-1}$	2.40×10^{-3}
(H24)	$Bcl_2 + Bax \underset{k_{-H24}}{\overset{k_{H24}}{\rightleftharpoons}} Bcl_2 : Bax$	$2.00 \times 10^{-4} nM^{-1} s^{-1}$	0.02
(H25)	$Bcl_2 + tBid \underset{k_{-H25}}{\overset{k_{H25}}{\rightleftharpoons}} Bcl_2 : tBid$	$2.00 \times 10^{-4} nM^{-1} s^{-1}$	0.02

978-1-4673-4398-5/12/$31.00 ©2012 IEEE

TABLE II
INITIAL CONCENTRATIONS OF EACH SPECIES IN THE ISS MODEL (HUA. ET AL. 2005)

Species	Initial concentration(nM)
Casp3	200.00
Bid	25.00
Bcl2	75.00
Bax	83.33
Cyto.c	100.00
Smac	100.00
XIAP	30.00
Casp9	20.00
ATP	10000.00
Apaf	100.00

for Apaf-1. Each element of the vector-valued function $Q(U)$ of U is the rate change of concentration to the corresponding species:

$$\begin{aligned} Q(U) = \quad & \big(-v_7 + v_8 - v_9 + v_{10} + v_0, v_7 - v_8, v_9 - v_{10}, \\ & -v_9, v_{10} - v_{11} - v_{25}, v_{11} - v_{12}, v_{12}, v_{25}, \\ & -v_{11} - v_{12} - v_{24}, v_{24}, -v_{24} - v_{25}, -v_{15}, \\ & v_{15} - v_{16}, v_{16} - v_{17}, v_{17} - v_{18} + v_{19}, v_{18} - v_{19}, \\ & -v_{16}, v_{19} - v_{20} + v_{21}, -v_{17} - v_{18} - v_{22}, \\ & -v_7 - v_{20}, v_{20} - v_{21}, v_8 + v_{21} - v_{23}, -v_{13}, \\ & v_{13} - v_{14}, -v_{14} - v_{22} - v_{23}, v_{14}, v_{22}, v_{23} \big)^T, \end{aligned}$$

where $v_i (i = 7 \cdots 25)$ is the rate of the i-th reaction in Table 1:

$$\begin{aligned} v_7 = \quad & k_{H7}[Casp8_2^*][Casp3] - k_{-H7}[Casp8_2^* : Casp3], \\ v_8 = \quad & k_{H8}[Casp8_2^* : Casp3], \\ v_9 = \quad & k_{H9}[Casp8_2^*][Bid] - k_{-H9}[Casp8_2^* : Bid], \\ v_{10} = \quad & k_{H10}[Casp8_2^* : Bid], \\ v_{11} = \quad & k_{H11}[tBid][Bax] - k_{-H11}[tBid : Bax], \\ v_{12} = \quad & k_{H12}[tBid : Bax][Bax] - k_{-H12}[tBid : Bax_2], \\ v_{13} = \quad & k_{H13}[Smac][tBid : Bax_2], \\ v_{14} = \quad & k_{H14}[Smac^*][XIAP] - k_{-H14}[Smac^* : XIAP], \\ v_{15} = \quad & k_{H15}[Cyto.c][tBid : Bax_2], \\ v_{16} = \quad & k_{H16}[Cyto.c^*][Apaf][ATP] \\ & \quad -k_{-H16}[Cyto.c^* : Apaf : ATP], \\ v_{17} = \quad & k_{H17}[Cyto.c^* : Apaf : ATP][Casp9] \\ & \quad -k_{-H17}[Cyto.c^* : Apaf : ATP : Casp9], \\ v_{18} = \quad & k_{H18}[Cyto.c^* : Apaf : ATP : Casp9][Casp9] \\ & \quad -k_{-H18}[Cyto.c^* : Apaf : ATP : Casp9_2], \\ v_{19} = \quad & k_{H19}[Cyto.c^* : Apaf : ATP : Casp9_2], \\ v_{20} = \quad & k_{H20}[Casp9^*][Casp3] - k_{-H20}[Casp9^* : Casp3], \\ v_{21} = \quad & k_{H21}[Casp9^* : Casp3], \\ v_{22} = \quad & k_{H22}[Casp9][XIAP] - k_{H-22}[Casp9 : XIAP], \\ v_{23} = \quad & k_{H23}[Casp3^*][XIAP] - k_{-H23}[Casp3^* : XIAP], \\ v_{24} = \quad & k_{H24}[Bcl_2][Bax] - k_{-H24}[Bcl_2 : Bax], \\ v_{25} = \quad & k_{H25}[Bcl_2][tBid] - k_{-H25}[Bcl_2 : tBid], \end{aligned}$$

v_0 is a constant rate of generation for $Casp8_2^*$ from the upstream process and its value was suggested in [30] as $v_0 = 0.001 nM s^{-1}$. Note that none of the reactions will occur if $Casp8_2^*$ has no a source. In addition, the non-zero initial concentrations for U are taken as in [9], [30] and are given in Table II.

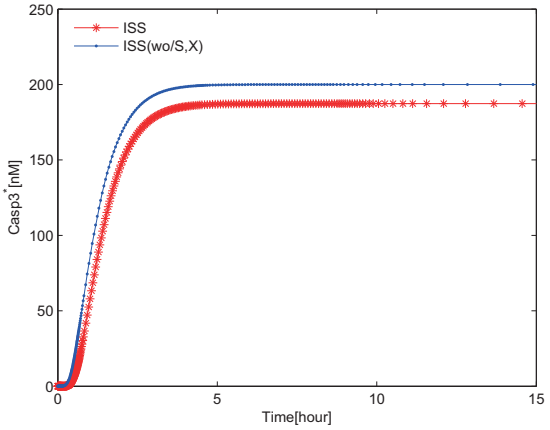

(a) Casp3* as a function of time t

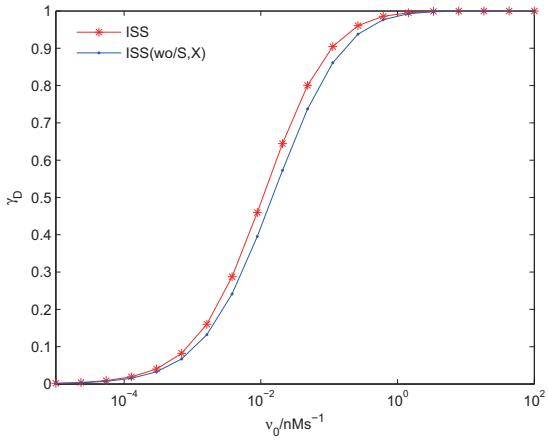

(b) γ_D as a function of the generation rate v_0

Fig. 2. Comparison of the ISS model(red asterisk) and the ISS(wo/S,X) model (blue dot). The initial concentrations are from Table. II. (a): Casp3* as a function of time t. (b): γ_D as a function of the generation rate v_0

With the above data, Okazaki et al. [30] investigated the M-D transition behavior of the ISS and ISS(wo/S,X) (without Smac and XIAP). Namely, when a large amount of $Casp8_2^*$ is activated from upstream, it will directly induce cell death through the D-channel; otherwise, the M-channel plays more important role for cell death. In doing this, they introduced a quantity γ_D to characterize the net production rate of Casp3* by the D-channel. By numerical simulations, they claimed that Smac and XIAP have little effect on the reaction process of the ISS and therefore they did not consider the related reactions in their simplification. We repeat their numerical results (see Fig. 2) and agree with that their claim is reasonable for the above data.

However, with different initial concentrations we get different results by solving the two systems numerically. Fig. 3 displays the result with the initial value of [Bax] divided by

978-1-4673-4398-5/12/$31.00 ©2012 IEEE

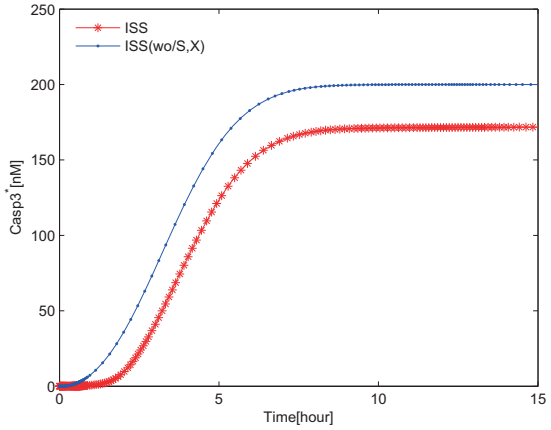

(a) Casp3* as a function of time t

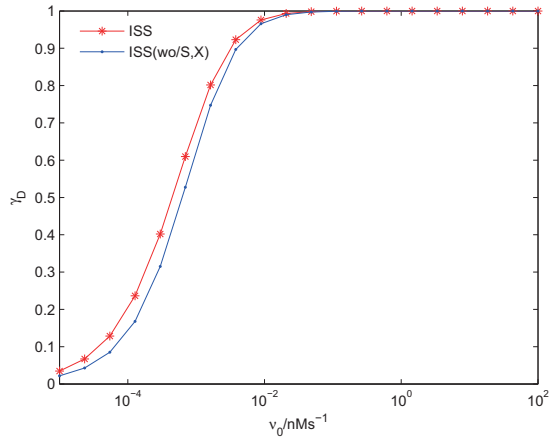

(b) γ_D as a function of the generation rate v_0

Fig. 3. Comparison of the ISS model(red asterisk) and the ISS(wo/S,X) model (blue dot) with the initial value of $[Bax]$ being that in Table 2 divided by 10 and others unchanged. (a): Casp3* as a function of time t. (b): γ_D as a function of the generation rate v_0

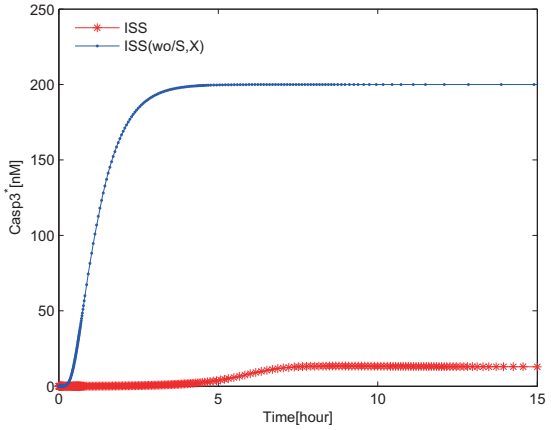

(a) Casp3* as a function of time t

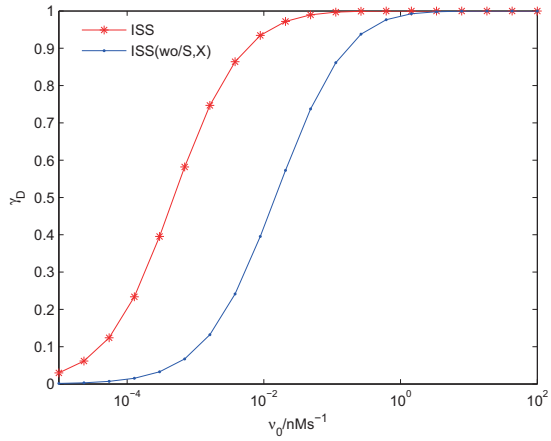

(b) γ_D as a function of the generation rate v_0

Fig. 4. Comparison of ISS model(red asterisk) and ISS(wo/S,X) model (blue dot) with the initial value of $[XIAP]$ being that in Table 2 multiplied by 10 and others unchanged. (a): Casp3* as a function of time t. (b): γ_D as a function of the generation rate v_0

10 and others kept as in Table 2, while the curves in Fig. 4 are those with the initial value of [XIAP] multiplied by 10 and others kept as in Table 2. Both Fig. 3 and Fig. 4 show that the ISS(wo/S,X) model is different from the ISS model. We have tested many sets of initial data and most of the numerical results confirm the difference. In conclusion, Smac and XIAP should not be ignored and our simplification will base on the entire ISS system.

III. Simplification

In this section we derive our simplified model by using the singular perturbation theory [27], [29] to the system of 28 ODEs (2.1).

Motivated by the simplification process in [30], we regard the six reversible reactions (H11), (H12), (H16), (H17), (H24) and (H25) in Table 1 as fast and the rest as slow. Accordingly, we decompose the concentration vector U as

$$U = \begin{pmatrix} X \\ Y \\ Z \end{pmatrix},$$

with X the products of the six reactions, Y the reactants and Z the rest:

$$\begin{aligned} X = \; & \big([tBid : Bax], [tBid : Bax_2], [Bcl_2 : tBid], \\ & [Bcl_2 : Bax], [Cyto.c^* : Apaf : ATP], \\ & [Cyto.c^* : Apaf : ATP : Casp9]\big)^T, \\ Y = \; & \big([tBid], [Bax], [Bcl_2], [Cyto.c^*], [Apaf], [Casp9]\big)^T, \\ Z = \; & \big([Casp8_2^*], [Casp8_2^* : Casp3], [Casp8_2^* : Bid], [Bid], \\ & [Cyto.c], [Cyto.c^* : Apaf : ATP : Casp9_2], \\ & [Casp9^*], [Casp3], [Casp9^* : Casp3], [Casp3^*], \\ & [Smac], [Smac^*], [XIAP], [Smac^* : XIAP], \\ & [Casp9 : XIAP], [Casp3^* : XIAP]\big)^T. \end{aligned} \tag{2}$$

978-1-4673-4398-5/12/$31.00 ©2012 IEEE

With this decomposition, the kinetic equations in (1) can be rewritten as

$$\begin{aligned}\frac{dX}{dt} &= \frac{1}{\varepsilon}\hat{Q}_1(X,Y) + Q_1(X,Y,Z),\\ \frac{dY}{dt} &= \frac{1}{\varepsilon}\hat{Q}_2(X,Y) + Q_2(X,Y,Z),\\ \frac{dZ}{dt} &= Q_3(X,Y,Z).\end{aligned} \tag{3}$$

Here ε is a small positive parameter characterizing the fastness,

$$\begin{aligned}\hat{Q}_1(X,Y) = &\ \varepsilon\big(v_{11}-v_{12}, v_{12}, v_{25}, v_{24}, v_{16}-v_{17}, v_{17}\big),\\ \hat{Q}_2(X,Y) = &\ \varepsilon\big(-v_{11}-v_{25}, -v_{11}-v_{12}-v_{24},\\ &\ -v_{24}-v_{25}, -v_{16}, -v_{16}, -v_{17}\big)^T\end{aligned}$$

stand for the rates of concentration change due to the rapid reactions, and

$$\begin{aligned}Q_1(X,Y,Z) = &\ \big(0,0,0,0,0,-v_{18}+v_{19}\big)^T,\\ Q_2(X,Y,Z) = &\ \big(v_{10},0,0,v_{15},0,-v_{18}-v_{22}\big)^T,\\ Q_3(X,Y,Z) = &\ \big(-v_7+v_8-v_9+v_{10}, v_7-v_8, v_9-v_{10},\\ &\ -v_9, -v_{15}, v_{18}-v_{19}, v_{19}-v_{20}+v_{21},\\ &\ -v_7-v_{20}, v_{20}-v_{21}, v_8+v_{21}-v_{23},\\ &\ -v_{13}, v_{13}-v_{14}, -v_{14}-v_{22}-v_{23}, v_{14},\\ &\ v_{22}, v_{23}\big)^T\end{aligned}$$

represent those from the slow reactions. Note that $\hat{Q}_1(X,Y)$ is same as $Q_i(X,Y,Z)(i=1,2,3)$ in order of magnitude. It is direct to check that

$$\hat{Q}_2(X,Y) + C\hat{Q}_1(X,Y) \equiv 0 \tag{4}$$

with C the following constant 6x6-matrix

$$C = \begin{pmatrix} 1 & 1 & 1 & 0 & 0 & 0\\ 1 & 2 & 0 & 1 & 0 & 0\\ 0 & 0 & 1 & 1 & 0 & 0\\ 0 & 0 & 0 & 0 & 1 & 1\\ 0 & 0 & 0 & 0 & 1 & 1\\ 0 & 0 & 0 & 0 & 0 & 1 \end{pmatrix}.$$

Notice that the six fast reactions are reversible and, as a whole, they obey the principle of detailed balance. In fact, it is clear that $\hat{Q}_1(X,Y) = 0 = \hat{Q}_2(X,Y)$ are equivalent to $v_{11} = v_{12} = v_{16} = v_{17} = v_{24} = v_{25} = 0$. Recall that

$$\begin{aligned}v_{11} = &\ k_{H11}[tBid][Bax] - k_{-H11}[tBid:Bax],\\ v_{12} = &\ k_{H12}[tBid:Bax][Bax] - k_{-H12}[tBid:Bax_2],\\ v_{16} = &\ k_{H16}[Cyto.c^*][Apaf][ATP]\\ &\ -k_{-H16}[Cyto.c^*:Apaf:ATP],\\ v_{17} = &\ k_{H17}[Cyto.c^*:Apaf:ATP][Caps9]\\ &\ -k_{-H17}[Cyto.c^*:Apaf:ATP:Casp9],\\ v_{24} = &\ k_{H24}[Bcl_2][Bax] - k_{-H24}[Bcl_2:Bax],\\ v_{25} = &\ k_{H25}[Bcl_2][tBid] - k_{-H25}[Bcl_2:tBid].\end{aligned} \tag{5}$$

Then for any given

$$Y = \big([tBid],[Bax],[Bcl_2],[Cyto.c^*],[Apaf],[Casp9]\big)^T$$

with all six components positive, we can use (5) to get

$$\begin{aligned}X = &\ \big([tBid:Bax],[tBid:Bax_2],[Bcl_2:tBid],\\ &\ [Bcl_2:Bax],[Cyto.c^*:Apaf:ATP],\\ &\ [Cyto.c^*:Apaf:ATP:Casp9]\big)^T,\end{aligned}$$

with all six components positive, such that $v_{11} = v_{12} = v_{16} = v_{17} = v_{24} = v_{25} = 0$. Therefore, the principle of detailed balance is verified.

Once the principle of detailed balance is verified, we know from [27] that the singular perturbation theory [29] of initial-value problems applies to the stiff system of ODEs in (3). In particular, the solutions to initial-value problems of (3) converge uniformly to those of a reduced system of ODEs, as ε goes to zero, in any bounded time interval away from zero.

In order to derive the reduced system, we refer to (4) and define

$$\tilde{Y} = Y + CX,$$

that is,

$$\begin{aligned}\tilde{Y} = &\ \big([tBid] + [tBid:Bax] + [tBid:Bax]\\ &\ +[Bcl_2:tBid],\\ &\ [Bax] + [tBid:Bax] + 2[tBid:Bax_2]\\ &\ +[Bcl_2:Bax],\\ &\ [Bcl_2] + [Bcl_2:tBid] + [Bcl_2:Bax],\\ &\ [Cyto.c^*] + [Cyto.c^*:Apaf:ATP]\\ &\ +[Cyto.c^*:Apaf:ATP:Casp9],\\ &\ [Apaf] + [Cyto.c^*:Apaf:ATP]\\ &\ +[Cyto.c^*:Apaf:ATP:Casp9],\\ &\ [Casp9] + [Cyto.c^*:Apaf:ATP:Casp9]\big)^T.\end{aligned}$$

Then the ODEs in (3) become

$$\begin{aligned}\frac{dX}{dt} &= \frac{1}{\varepsilon}\tilde{Q}_1(X,Y) + Q_1(X,Y,Z),\\ \frac{d\tilde{Y}}{dt} &= Q_2(X,Y,Z) + CQ_1(X,Y,Z),\\ \frac{dZ}{dt} &= Q_2(X,Y,Z).\end{aligned} \tag{6}$$

As ε goes to zero, $\tilde{Q}_1(X,Y)$ is forced to vanish, from which we get the following algebraic equations

$$\begin{cases} v_{11} = k_{H11}[tBid][Bax] - k_{-H11}[tBid:Bax] = 0,\\ v_{12} = k_{H12}[tBid:Bax][Bax] - k_{-H12}[tBid:Bax_2] = 0,\\ v_{16} = k_{H16}[Cyto.c^*][Apaf][ATP]\\ \quad -k_{-H16}[Cyto.c^*:Apaf:ATP] = 0,\\ v_{17} = k_{H17}[Cyto.c^*:Apaf:ATP][Caps9]\\ \quad -k_{-H17}[Cyto.c^*:Apaf:ATP:Casp9] = 0,\\ v_{24} = k_{H24}[Bcl_2][Bax] - k_{-H24}[Bcl_2:Bax] = 0,\\ v_{25} = k_{H25}[Bcl_2][tBid] - k_{-H25}[Bcl_2:tBid] = 0. \end{cases}$$

These algebraic equations can be easily solved as

$$[tBid:Bax] = \frac{k_{H11}[tBid][Bax]}{k_{-H11}} = K_{H11}[tBid][Bax],$$

978-1-4673-4398-5/12/$31.00 ©2012 IEEE

$$[tBid:Bax]=\frac{k_{H11}[tBid][Bax]}{k_{-H11}}=K_{H11}[tBid][Bax],$$

$$\begin{aligned}[Cyto.c^*:Apaf:ATP] &= \frac{k_{H16}[Cyto.c^*][Apaf][ATP]}{k_{-H16}}\\ &= K_{H16}[Cyto.c^*][Apaf][ATP],\end{aligned}$$

$$\begin{aligned}&[Cyto.c^*:Apaf:ATP:Casp9]\\ &\quad=\frac{k_{H17}[Cyto.c^*:Apaf:ATP][Casp9]}{k_{-H17}}\\ &\quad=K_{H17}K_{H16}[Cyto.c^*][Apaf][ATP][Casp9],\end{aligned}$$

$$[Bcl_2:Bax]=\frac{k_{H24}[Bcl_2][Bax]}{k_{-H24}}=K_{H24}[Bcl_2][Bax],$$

$$[Bcl_2:tBid]=\frac{k_{H25}[Bcl_2][tBid]}{k_{-H25}}=K_{H25}[Bcl_2][tBid]$$

with $K_{Hi}=k_{Hi}/k_{-Hi}$ for $i=11,12,16,17,24,25$. These relations can be written as $X=\Phi(Y)$.

Substituting $X=\Phi(Y)$ into the second and third equations in 6, we obtain

$$\begin{cases}\dfrac{d\tilde{Y}}{dt}=Q_2(\Phi(Y),Y,Z)+CQ_1(\Phi(Y),Y,Z),\\ \dfrac{dZ}{dt}=Q_3(\Phi(Y),Y,Z).\end{cases}$$

On the other hand, from $\tilde{Y}=Y+CX=Y+C\Phi(Y)$ we compute the time derivative of $\tilde{Y}$:

$$\frac{d\tilde{Y}}{dt}=\frac{dY}{dt}+C\Phi(Y)_Y\frac{dY}{dt},$$

where $\Phi(Y)_Y$ represents the Jacobian matrix of $\Phi(Y)$. Denote by I_6 the unit matrix of order 6. According to the general theory developed in [27], the 6x6-matrix $[I_6+C\Phi(Y)_Y]$ is always invertible. Thus we gain equations for Y:

$$\begin{aligned}\frac{dY}{dt} &= (I_6+C\Phi(Y)_Y)^{-1}\tfrac{d\tilde{Y}}{dt}\\ &= (I_6+C\Phi(Y)_Y)^{-1}(Q_2(\Phi(Y),Y,Z)\\ &\qquad +CQ_1(\Phi(Y),Y,Z)).\end{aligned}$$

Consequently, the original system of 28 ODEs is reduced to the following 22 ODEs

$$\begin{aligned}\frac{dY}{dt} &= (I_6+C\Phi(Y)_Y)^{-1}(Q_2(\Phi(Y),Y,Z)\\ &\qquad +CQ_1(\Phi(Y),Y,Z)),\\ \frac{dZ}{dt} &= Q_3(\Phi(Y),Y,Z)\end{aligned}\tag{7}$$

together with 6 algebraic relations

$$X=\Phi(Y).$$

Recall that Y and Z are defined in (2). This system of 22 ODEs is our simplified model—a preliminary simplification of the ISS model. From now on, we call this simplified model (7) as PSISS model.

IV. Simulation Results

In this section we report some numerical results to compare our PSISS model with the ISS model and Okaxaki et al.'s ISS skeleton model (See Table III). The calculations were done with Matlab.

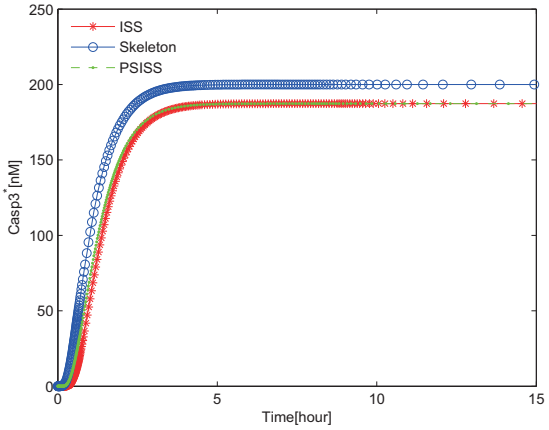

(a) The curves of Casp3* for 15 hours

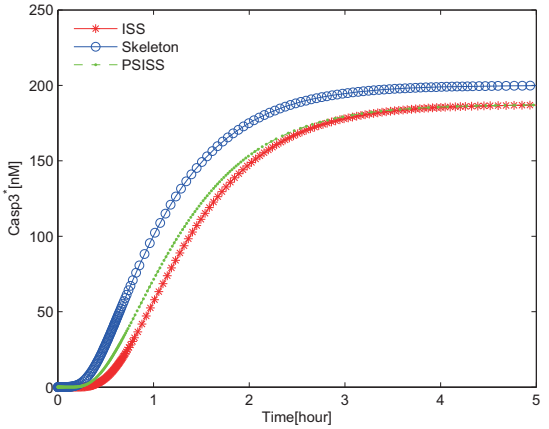

(b) The curves of Casp3* for 5 hours

Fig. 5. Comparison of the ISS model (red asterisk), the skeleton model (blue open circle) and our PSISS model (green dot). The initial concentrations are from Table II. (a): the curves of Casp3* for 15 hours. (b): the curves of Casp3* for 5 hours.

A. Accuracy of the PSISS model

As a first step, we compute the concentration of each species as functions of time t, with the initial concentrations from Table II, by using the entire ISS model, the ISS skeleton model and our PSISS model. Fig. 5 displays the curves for Casp3* as functions of time t. From these figures, especially Fig. 5(b), we see that the PSISS model and the ISS model give almost the same curves and equilibrium value for Casp3*, while what the skeleton model yields are different. This conclusion is further supported by the curves for other species. For example, we see Fig. 6 for the curves of Casp3 and Casp9* as functions of time t. These numerical results show that our PSISS model is closer to the original ISS model than the skeleton model.

B. M-D transition behavior

In Section 2, we have explained the M-D transition behavior and discussed the curves of γ_D as a function of the generation rate v_0 for the ISS model and the ISS(wo/S,X) model. Another

978-1-4673-4398-5/12/$31.00 ©2012 IEEE

TABLE III
THE ISS SKELETON MODEL DUE TO OKAZAKI ET AL. (2008)

Reaction		Rate constant
(S1)	$Casp8_2^* + Casp3 \longrightarrow Casp8_2^* + Casp3^*$	$6.25.00 \times 10^{-6} nM^{-1} s^{-1}$
(S2a)	$Casp8_2^* + Bid \longrightarrow Casp8_2^* + 0.0328tBid : Bax_2$	$v_{S2a} = \frac{k_a[Casp8_2^*][Bid]}{[Casp8_2^*]+K_a} (k_a = 0.1s^{-1}, K_a = 20nM)$
(S2b)	$Cyto.c + tBid : Bax_2 \longrightarrow 0.867Cyto.c^* : Apaf : ATP + tBid : Bax_2$	$1 \times 10^{-3} nM^{-1} s^{-1}$
(S2c)	$Cyto.c^* : Apaf : ATP + 2Casp9 \longrightarrow Cyto.c^* : Apaf : ATP + Casp9 + Casp9^*$	$1.46 \times 10^{-6} nM^{-1} s^{-1}$
(S2d)	$Casp9^* + Casp3 \longrightarrow Casp9^* + Casp3^*$	$1.96 \times 10^{-5} nM^{-1} s^{-1}$

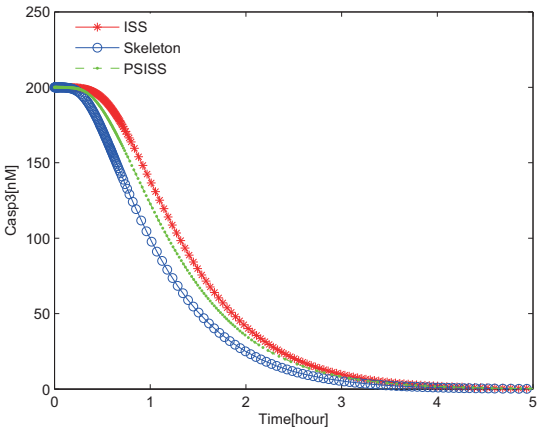

(a) The curves of Casp3 as functions of t

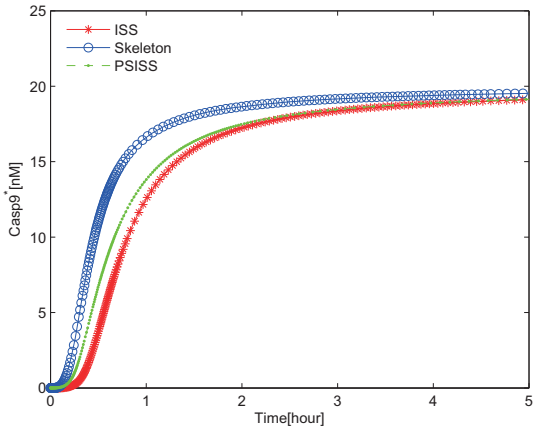

(b) The curves of Casp9* as functions of t

Fig. 6. Comparison of the ISS model (red asterisk), the skeleton model (blue open circle) and our PSISS model (green dot). (a): the curves of Casp3 as functions of t. (b): the curves of Casp9* as functions of t.

important observation related to the M-D transition behavior is that the initial concentration of Casp9 have a great impact to this behavior. To expose this observation, a new quantity v_0^C was introduced in [30] to represent the critical value of v_0 corresponding to $\gamma_D = 0.5$. By its definition, $\gamma_D = 0.5$ means that the effect of the M-channel is same as that of the D-channel.

Here we explore the M-D transition behavior of our PSISS model and compare it with the ISS and skeleton model on this property. To this end, we exhibit the results of the three models in Fig. 7(a). Moreover, the curves of v_0^C as a function of the initial concentration of Casp9 are shown in Fig. 7(b). These two figures show that our PSISS model is in a better agreement with the original ISS model than the skeleton model. In particular, Fig. 7(b) indicates that the PSISS model essentially improves the skeleton model for large initial concentrations of Casp9.

C. Sensitivity Analysis

In [9], Hua et al. used sensitivity analysis to show that increasing or decreasing the expression levels of a molecule can have an asymmetrical effects on the signaling outcome. The outcome they cared about is how fast Casp3 becomes activated and the half-time for activating Casp3 was used to quantify the outcome. Here we analyze the sensitivity of the ISS model, the skeleton model and our simplified model PSISS. What different from [9] is that our sensitivity analysis is only about the molecules in the downstream process. The baseline values of the species are those in Table II. The numerical results for the three models are shown in Fig. 8.

From Fig. 8, we see that our PSISS model is very similar to the ISS model, except a little difference for Bcl2. Though the half-time changes slightly for Bcl2, the asymmetry is preserved. Overall, our PSISS model behaves obviously better than the ISS skeleton model does.

As a new aspect of the sensitivity analysis for our simplification, we also examine the equilibrium values of Casp3*—the indicator of apoptosis, by changing the initial concentration of every species. From this purpose, we introduce a new quantity as follows

$$\alpha_{C3^*} = \frac{[Casp3^*] \ at \ equilibrium \ for \ PSISS}{[Casp3^*] \ at \ equilibrium \ for \ ISS}.$$

When initial concentrations of some species are changed, α_{C3^*} will likely change too. For a good simplified model, such a quantity should be close to one.

We compute α_{C3^*} from our PSISS model with initial concentrations changed for each species, including Casp3*. The result is given in Fig. 9, illustrating that α_{C3^*} is insensitive to most of initial concentration changes, except a little sensitivity for Bcl2 and Bax. In total, α_{C3^*} is almost free from the influence of the initial concentration changes. This further

978-1-4673-4398-5/12/$31.00 ©2012 IEEE

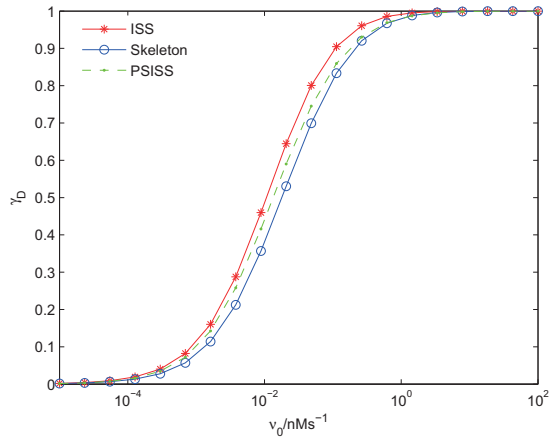

(a) M-D transition behaviors due to Casp8$^*_2$

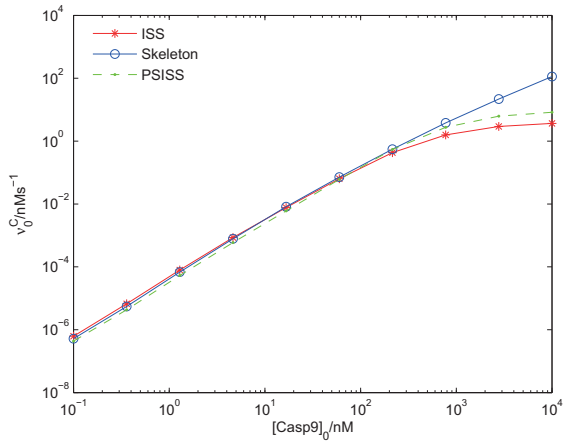

(b) M-D transition behaviors due to Casp9

Fig. 7. M-D transition comparison of the ISS model (red asterisk), the skeleton model (blue open circle) and the PSISS model (green dot). (a): M-D transition behavior due to Casp8$^*_2$. (b): M-D transition behavior due to Casp9.

reveals the reliability of our simplified model and the PEA method.

V. Conclusions

In this paper, we derive the PSISS model by strictly applying the PEA method to the ISS model proposed by Hua et al. (2005). Through numerical simulations, we compare this new model with the original ISS model and Okazaki et al.'s skeleton model from various aspects, including accuracy, sensitivity and M-D transition behavior. Moreover, we introduce a new quantity α_{C3^*} to evaluate the new model. All these numerical results show the reliability of both our simplified model and the PEA method.

The new simplified model consists of ODEs. It is desirable to write down the corresponding biochemical reactions and thereby provide a new understanding of the apoptosis mechanism.

The present simplification is preliminary and further results will be reported in a forthcoming paper. We believe that

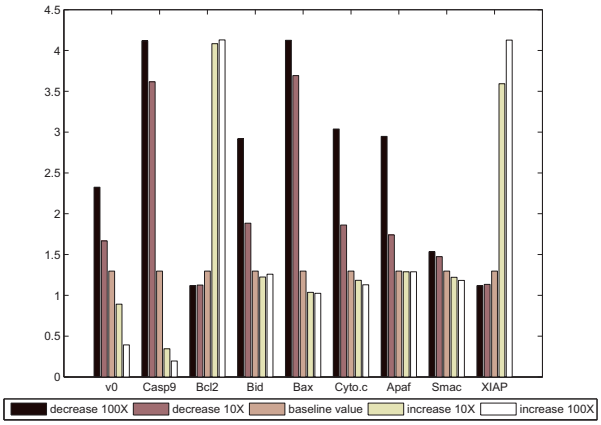

(a) Half-time for activating Casp3* with the ISS model

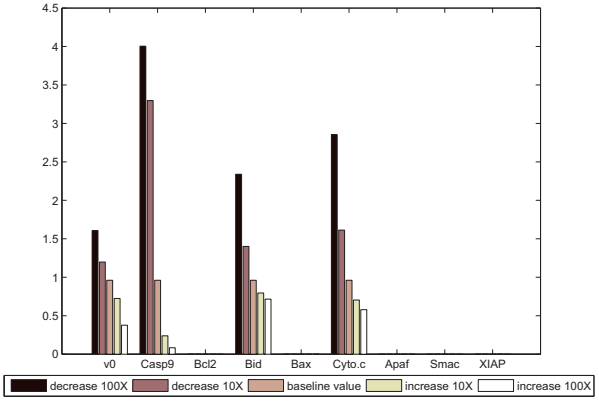

(b) Half-time for activating Casp3* with the skeleton model

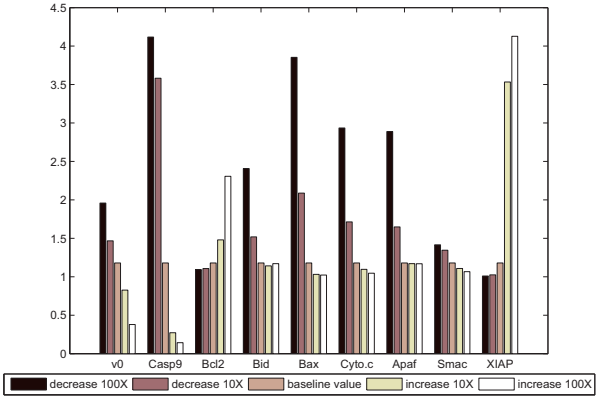

(c) Half-time for activating Casp3* with the PSISS model

Fig. 8. Sensitivity analysis of the ISS model, the skeleton model and the PSISS model. The overexpression or knockdown level of each species is changed one or two orders of magnitude while the others unchanged.

978-1-4673-4398-5/12/$31.00 ©2012 IEEE

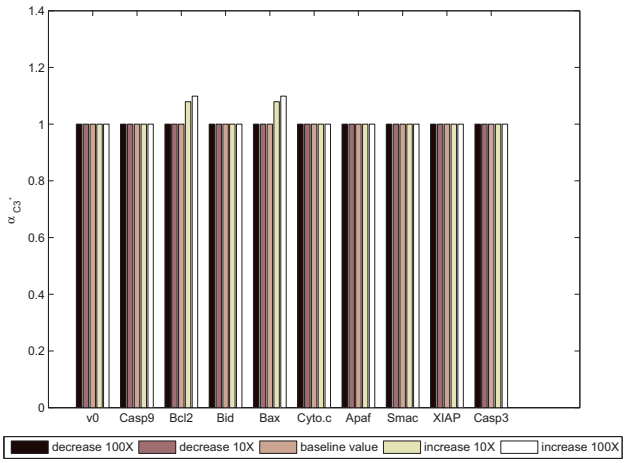

Fig. 9. The change of α_{C3^*} to different initial concentrations. The overexpression or knockdown level of each species is changed one or two orders of magnitude once while the others unchanged.

the framework presented here is useful for simplifying other biochemical systems as well as the apoptosis problem.

ACKNOWLEDGMENT

This work was partially supported by the National Natural Science Foundation of China (NSFC 10971113). The authors are grateful to Mr. Chang GU for many valuable discussions at the beginning of this project.

REFERENCES

[1] M. O. Hengartner, *The Biochemistry of apoptosis*, Nature 407 (2000), 770–776.
[2] H. R. Horvitz, *Genetic Control of Programmed Cell Death in the Nematode Caenorhabditis elegans*, Cancer Res. 59 (1999), 1701–1706.
[3] C. B. Thompson, *Apoptosis in the pathogenesis and treatment of disease*, Science 267(1995), 1456–1462.
[4] M. Raff, *Cell suicide for beginners*, Nature 396(1998), 119–122.
[5] P. Meier, A. Finch, and G. Evan, *Apoptosis in development*, Nature 407(2000), 796–801.
[6] I. N. Lavrik, R. Eils, N. Fricker, C. Pforr, and P.H. Krammer, *Understanding apoptosis by systems biology approaches*, Mol. BioSyst. 5(2009), 1105–1111.
[7] A. Ashkenazi and V. M. Dixit, *Death receptors: signaling and modulation*, Science 281(1998), 1305–1308.
[8] J. Schmitz, S. Kirchhoff, and P. H. Krammer, *Regulation of death receptor-mediated apoptosis pathways*, Int. J. Biochem. Cell Biol. 32(2000), 1123–1136.
[9] F. Hua, M. G. Cornejo, M. H. Cardone, C. L. Stokes, and D. A. Lauffenburger, *Effects of Bcl-2 levels on Fas signaling-induced Caspase-3 activation: molecular genetic tests of computational model predictions*, J. Immunol. vol. 175(2005), 985–995.
[10] B. C. Barnhart, E. C. Alappat, and M. E. Peter, *The CD95 type I/type II model*, Semin. Immunol. 15(2003), 185–193.
[11] A. K. Samraj, E. Keil, N. Ueffing, K. Schulze-Osthoff, and I. Schmitz, *Loss of caspase-9 provides genetic evidence for the type I/II concept ofCD95-mediated apoptosis*, J. Biol. Chem. 281(2006), 29652–29659.
[12] C. Scaffidi, S. Fulda, A. Srinivasan, C. Friesen, F. Li, K. J. Tomaselli, K. M. Debatin, P. H. Krammer, and M. E. Peter, *Two CD95 (APO-1/Fas) signaling pathways*, EMBO J. 17(1998), 1675–1687.
[13] J. Keener and J. Sneyd, *Mathematical Physiology*, Springer, 1998.
[14] D. L. Chapman and L. K. Underhill, *The interaction of chlorine and hydrogen. The influence of mass*, J. Chem. Soc. Trans. 103(1913), 496–508.
[15] S. W. Benson, *The Foundations of Chemical Kinetics*, McGraw-Hill, New York, 1960.
[16] J. R. Bowen, A. Acrivos and A. K. Oppenheim, *Singular perturbation refinement to quasi-steady state approximation in chemical kinetics*, Chem. Eng. Sci. 18(1963), 177–188.
[17] P. Karlson, *Introduction to Modern Biochemistry*, Academic, New York, 1967.
[18] S. J. Fraser, *The steady state and equilibrium approximations: A geometrical picture*, J. Chem. Phys. 88(1988), 4732–.
[19] M. Rein, *The partial-equilibrium approximation in reacting flows*, Physics of Fluids A: Fluid Dynamics, 4(1992), 873–886.
[20] G. E. Briggs and J. B. S. Haldane, *A Note on the Kinetics of Enzyme Action*, Biochem J. 119(1925), 338–339.
[21] D. A. Goussis and U. Maas, *Model Reduction for Combustion Chemistry*, Turbulent Combustion Modeling, 95 (2011), 193–220.
[22] N. Peters, *Numerical and Asymptotic Analysis of Systematically Reduced Reaction Schemes for Hydrocarbon Flames*, In: R.G. et al. (ed.) Lecture Notes in Physics, pp. 90C109. Springer-Verlag, Berlin/New York, 1985.
[23] M. D. Smooke,(ed.) *Reduced Kinetic Mechanisms and Asymptotic Approximations for Methane-Air Flames*, Lecture Notes in Physics 384, Springer, Berlin, Heidelberg, New York, 1991.
[24] J. D. Ramshaw, *Partial chemical equilibrium in fluid dynamics*, Phys. Fluids 23(1980), 675–.
[25] C. C. Lin and L. A. Segel, *Mathematics applied to deterministic problems in the natural sciences*, Macmillan, 1974.
[26] D. F. Walls, H. J. Carmichael, R. F. Gragg and W. C. Schieve *Detailed balance, Liapounov stability, and entropy in resonance fluorescence*, Phys. Rev. A 18(1978), 1622–1627.
[27] W. A. Yong, *An interesting class of partial differential equations*, J. Math. Phys. 49(2008), 033503–.
[28] J. D. Murray, *Asymptotic Analysis*, Springer, New York, 1984.
[29] W. A. Yong, *Singular perturbations of first-order hyperbolic systems with stiff source terms*, J. Differ. Eqns. 155(1999), 89–132.
[30] N. Okazaki, R. Asano, T. Kinoshita, and H. Chuman, *Simple computational models of type I/type II cells in Fas signaling-induced apoptosis*, J Theor. Biol. 250(2008), 621–633.

978-1-4673-4398-5/12/$31.00 ©2012 IEEE